

ATTACHMENT 1

ARTECH TESTING L.L.C.
FINAL REPORT



ARTECH TESTING, L.L.C.

14554 LEE ROAD • CHANTILLY, VA 20151-1632
703 378-7263 • 800 283-7848 • FAX 703 378-7274

TWA FLIGHT 800 WRECKAGE EXAMINATION

PRODUCT TESTING

.....

FAILURE ANALYSIS

.....

LITIGATION SUPPORT

.....

CHEMICAL ANALYSIS

.....

ENGINEERING
CONSULTING

.....

MATERIALS RESEARCH

.....

BIO-MATERIALS

.....

FOOTWEAR TESTING

**Prepared for
PERKINS COIE LLP,
KREINDLER & KREINDLER,
and
NATIONAL TRANSPORTATION SAFETY BOARD**

**Prepared by
V. Sahay, Principal Metallurgical Engineer
Craig Nelsen, Chemist**

**ARTECH Testing, LLC
Project No. M90127
December 22, 1999**

INTRODUCTION

Two sections of the fuel tank and several pieces of the scavenge pump inlet tube of the TWA Flight 800 were provided to ARTECH Testing, LLC for examination in accordance with the attached test protocol. All laboratory examinations were performed in the presence of the parties involved in the litigation case. This report summarizes the findings of the laboratory examination.

FUEL TANK SECTIONS

VISUAL EXAMINATION

Two sections of the tank are shown in figures 1 and 2 in the as-received condition. The approximate dimensions of Sections CW236 and CW238 were 30x15 inches and 10x8 inches respectively. Both sections were deformed as shown in the photographs. The fracture plane along which these sections had fractured is shown in figure 3.

Enlarged views of the inside and outside surfaces of the hole in Section CW236 are shown in figure 4. As indicated in figure 5, a major part of the tank material around the hole exhibited features of outward deformation.

Enlarged views of the fracture surface of the Section CW238 adjacent to the hole are shown in figures 6A and 6B. Note the flattening damage at the lip of the fracture surface on the inside surface of the tank; a light brown stain was also observed on the fracture surface in that area. A deep gouge/dent mark, about 1.5 inches long, was noticed on the inside surface of the tank; its location in reference to the hole is indicated in figure 2A. It appeared as if a foreign object had penetrated the tank material inside out.

Profile of the hole in reference to the inside and outside surfaces of the tank was traced on a transparent paper. Measurements at different locations were taken using a calibrated digital caliper. See figure 7 for details. Thickness of the tank material near the fracture surface was in the range of 0.2965-0.3080 inches and that remote from the fracture surface was 0.3060-0.3088 inches. All measurements were taken without removing the paint.

CHEMICAL ANALYSIS

Cotton swabs soaked in Methylene Chloride were used to collect samples by wiping any debris, soot or deposits from the fracture surfaces. The samples were stored in clean glass vials. The collected samples were identified as follows:

Sample CW236 – 1 : By wiping on the fracture surface around the hole.

Sample CW238 – 1 : By wiping on the fracture surface in a clean area remote from the hole location (away from the stained area).

Sample CW238 – 2 : By wiping on the fracture surface in the stained area.

Fourier Transform Infrared Spectroscopy (FTIR)

Samples CW236 - 1, CW238 - 1, and CW238-2 were analyzed by FTIR using Sodium Chloride plates. Sodium Chloride crystals, due to their structure and chemical bonding,

are "invisible" to FTIR analysis. These salt plates are employed in FTIR whenever liquid samples are examined. A couple of drops of Methylene Chloride were placed on these plates and used as a background spectrum. A similar quantity of the sample was retrieved from Sample CW238-1 (the reference area wet swab) and was examined. It was found to have a flat baseline with some negative peaks. This is an indication that the blank did not contain any foreign contaminants and was useful as a reference. The analysis of Sample CW238-2 did not show any measurable absorbance. Some slight baseline disturbances were noticed in the region from 2800-3000 wavenumbers. The analysis of Sample CW236 - 1 yielded no matches when examined against the computer database. However, it did have absorbances in the region around 2800-3100 wavenumbers. This region is an area in which hydrocarbons are active. While FTIR was unable to identify any exact compound in CW236 - 1, it suggested that hydrocarbons were present. This information became useful in conjunction with the results of the GC-MS analysis.

The results of FTIR analysis of Samples CW236 - 1, CW238 - 1 and CW238 - 2 did not yield any identifiable compounds or contaminants. However, a trace of hydrocarbons was detected in Sample CW236 - 1. All FTIR spectra are attached in Appendix 1

Gas Chromatography-Mass Spectrometry (GC-MS)

The samples were further analyzed by GC-MS. Before analyzing the samples, the GC-MS system was auto-calibrated. Using a syringe, about 2 microliters of sample solution was retrieved from each sample vial for analysis. The syringe containing the sample was placed into the GC-MS injection port and inserted through a rubber septum. It was then injected and the instrument was started. Analysis runs were 45 minutes per sample. Once complete, the computer was used to automatically examine each peak present in a spectrum and determine the top three candidates for each peak. All GC-MS spectra are attached in Appendix 2

Based on the test results, the following conclusions can be made:

- 1) The analysis of blanks associated with the testing of Sections CW236 and CW238 yielded a spectrum devoid of compounds save for Methylene Chloride. The blank for Section CW236 was a swab soaked in Methylene Chloride and the blank for Section CW238 was Sample CW238 - 1. These negative results were expected and proper.
- 2) The analysis of Sample CW236 yielded six peaks of notice. These peaks were associated with long-chain branched hydrocarbons and Poly-Aromatic Hydrocarbons (PAHs).
- 3) The analysis of Sample CW238 - 2 yielded five peaks of notice. These peaks were associated with Poly-Aromatic Hydrocarbons (PAHs), such as Perylene d12.
- 4) In reference to these conclusions, all samples had signs of hydrocarbon combustion. This is indicated by the presence of PAHs and long-chain

branched hydrocarbons. This conclusion is expected in the subject fuel tank sections.

FRACTURE SURFACE EXAMINATION

Small parts of fracture surfaces were cut from Sections CW236 and CW238 for examination by optical microscopy and Scanning Electron Microscopy – Energy Dispersive Spectroscopy (SEM – EDS).

EDS Analysis of Section CW236

Since the tank section CW236 was large in size, three small sections, identified as 1; 2; and 3, were cut from various locations around the hole to perform fracture surface examination; those locations are shown in figure 8. Section 3 was further cut in two parts, 3A and 3B, for easy access to the fracture area of interest. See figure 9. All cuts were made dry using a band saw. Most of the fracture surface appeared featureless under an optical microscope. Section 1 exhibited a two-step fracture feature where it appeared as if some hard foreign object had penetrated about halfway through its thickness from the inside surface of the tank material, followed by failure of the remaining ligament (figure 10).

Different locations of the fracture surface of each small section were analyzed by EDS; all collected EDS spectra are attached in Appendix 3. The results are as follows:

Section CW236 – 1: Two EDS spectra were collected from different locations on the fracture surface. Both spectra indicated major peaks of Aluminum (Al), Copper (Cu), Chlorine (Cl), Sulfur (S) and Calcium (Ca). Minor presence of Magnesium (Mg), Manganese (Mn), Iron (Fe), Sodium (Na) and Potassium (K) was also detected. The presence of Al, Cu, Mg, and Mn is attributed to the tank materials, which is probably made from a 2000 series aluminum alloy. The most likely source of S is the fuel and that for Cl and Na is the seawater. Other elements found on the surface are due to some foreign deposit.

Section CW236 – 2: Three EDS spectra were collected from different locations on the fracture surface. The result was similar to what was detected on Section CW236 – 1.

Section CW236 – 3: Two EDS spectra were collected from different locations on the fracture surface. The result was similar to what was detected on Section CW236 – 1. In addition, Silicon (Si) was also detected.

EDS Analysis of Section CW238

A 0.5x2.5 inch section was cut from Section CW238 as indicated in figure 11; this section was adjacent to the hole in Section CW236. The cut was made dry by using a band saw. Both stained area (shown in figure 6A) and an area remote from stained area

(shown in figure 6B) were analyzed by EDS. Two EDS spectra collected from the stained area indicated major peaks of Al, Cu, Cl, and S. Minor presence of K, Ca, Fe, and Phosphorus (P) was also detected. Similar results were obtained from the unstained area. See the EDS spectra in Appendix 3. These results are similar to what was found in Section CW236 analysis.

Fractography of Sections CW236 and CW238

Subsequent to EDS analysis, the small sections cut from Sections CW236 and CW238 were cleaned in toluene and acetone sequentially for 5 minutes each in an ultrasonic bath. Cleaned and dried sections were examined by SEM. Since the fracture surfaces were badly corroded, the mode of failure could not be determined. These sections were further cleaned in a 5% solution of ALCONOX (detergent) in an ultrasonic bath for another 10 minutes followed by rinsing in de-ionized water and drying in acetone.

In spite of extended solvent cleaning, most of the fracture surfaces were found to be covered with corrosion product which made it impossible to characterize the fracture mode as shown in figure 12 for Section CW236 - 1. A few patches of clean areas in Section CW236 - 2 revealed a featureless surface (figure 13); the original fracture surface may have been rendered featureless due to corrosion attack. Areas on the inside surface of the tank immediately adjacent to the fracture surface exhibited cracks in the paint layer, which are typically formed due to tensile load (figure 14). In this case, the likely source of tensile load was a hard object pushing through the inside surface, creating the subject hole. Fracture surfaces in Section CW236 - 3A and CW236 - 3B exhibited similar features as seen in Section - 2 (figures 15 and 16).

The fracture surface of Section CW238 revealed the presence of extensive amounts of corrosion product, which made it impossible to characterize the fracture surface; see figure 17.

The results of fractography were not conclusive because the fracture surfaces were covered with adherent corrosion deposits.

METALLOGRAPHIC EXAMINATION

One transverse section through the fracture face was cut from each of Sections CW236 - 1, CW236 - 2, CW236 - 3A, CW236 - 3B, and CW238. The section locations are shown in figures 18 and 19. These sections were prepared for metallographic analysis. The fracture faces of the polished and etched sections were examined at various magnifications to characterize the direction of grain flow. Photomicrographs of the sections are presented in figures 20-24. Grain flow in these photomicrographs clearly indicates stretching of grains from the inside surface of the tank to the outside surface.

This feature suggests that the damage to the tank initiated on the inside surface and propagated outwardly. No evidence of recrystallized grains and/or incipient melting at the fracture surfaces was observed which precludes high strain rate impact preceding formation of the hole. Some areas on the inside and the outside surfaces of the tank exhibited features typical of intergranular corrosion; see figures 20A, 22A, 23A, and 24A.

The results of metallographic analysis suggest that a slowly applied load on the inside surface created the hole in the tank.

SCAVENGE PUMP INLET TUBE

CHEMICAL ANALYSIS

Pieces of the scavenge pump inlet tube are shown in figure 25. Tube sections, which had been cut longitudinally in half, were identified as 65B and S3052 (figure 26).

Cotton swabs were used to collect samples by wiping any debris, soot or deposits from the inside surfaces of the tubes. The following samples were collected from the tube sections:

- Two dry swab samples collected from each tube as indicated in figure 27.
Dry Sample ID: 65B-A & B, S3052-A & B.
- Two wet swab samples (using Methylene Chloride soaked swabs) collected from each tube as shown in figure 28.
Wet Sample ID: 65B-A & B, S3052-A & B.

ARTECH analyzed dry samples 65B-B and S3052-B along with a standard (unused) swab on November 4, 1999. The remaining dry samples and all wet samples were withheld by NTSB for future analysis.

FTIR Analysis

An Attenuated Total Reflection (ATR) adapter was employed to augment the FTIR analysis. This allowed the sample surface of the dry swabs to be analyzed. The unused cotton swab was examined and used as the background for the analysis of the samples. The analysis of both dry samples, 65B-B and S3052-B, yielded reproducible results. These results were searched against a computer database of nearly 15,000 compounds. The analysis of Sample 65B-B, which was analyzed three times, returned no results of a suitable confidence level. Therefore, the analysis of Sample 65B-B is inconclusive. The analysis of Sample S3052-B, which was analyzed four times, yielded no matches of a reliable rating. However, a compound "Viton" was given a low confidence (< 35%) match; this type of low level match is not of a suitable confidence level. Therefore, the analysis of Sample S3052-B is also inconclusive.

Given the amplitude of absorbance gained from these dry swabs, inconclusive analysis is not surprising. The overall amplitude of these reading was less than 0.03 AU (Absorbance Units, 3% full scale) at their maximum in Sample S3052-B, and the more typical absorbance was less than 1% full scale. The absorbance reading from Sample 65B-B was worse. Although the peak near 2400 wavenumbers seems to be nearly 10% full scale, this is a sign of atmospheric carbon dioxide, an unavoidable background noise.

Based on these results, it is concluded that the results of FTIR analysis of dry swab samples 65B-B and S3052B-B are inconclusive. All FTIR spectra are attached in Appendix 1.

GC-MS Analysis

NTSB returned wet swab samples 65B-B and S3052-B to ARTECH on November 8, 1999. The samples were stored in a refrigerator for analysis at a later date. Per agreement of the concerned parties, these samples were analyzed on November 12, 1999 in the presence of the representatives of the law offices of Kreindler & Kreindler and Dombroff & Gilmore.

Fluid samples from the vials were collected in the same way as was done for the wet swab samples of the fuel tank sections described earlier. However, the Methylene Chloride solvent in one sample (65B-B) had evaporated. The cause of this was unknown. Upon agreement of the above mentioned law firms, the sample was reconstituted with the addition of 1.0 milliliter of Methylene Chloride. The samples were analyzed as described earlier. All GC-MS spectra are attached in Appendix 2.

The collected data for all the samples was analyzed and reviewed. From this analysis, the following conclusions can be made:

- 1) The analysis of the cotton swab used as a reference returned a spectrum devoid of any peaks, except for Methylene Chloride.
- 2) The analysis of 65B-B yielded seven peaks of notice. These peaks were associated with long-chain branched hydrocarbons and Poly-Aromatic Hydrocarbons (PAHs). There were also signs of hydrocarbon chains that incorporated poly-substituted benzyl and phenyl ring systems.
- 3) The analysis of S3052-B yielded seven peaks of notice. These peaks were associated with long-chain branched hydrocarbons and Poly-Aromatic Hydrocarbons (PAHs). There were also signs of hydrocarbon chains that incorporated poly-substituted benzyl and phenyl ring systems.
- 4) In reference to these conclusions, two possible scenarios can explain the presence of the unusually long hydrocarbon chains, PAHs, and benzyl/phenyl compounds:

- A) These products are the results of hydrocarbon combustion. The presence of PAHs and long-chain branched hydrocarbons is an indicator of this. Further, the presence of substituted phenyl and benzyl hydrocarbons, in addition to PAHs and long-chained branched hydrocarbons, indicates that the combustion of those hydrocarbons was an oxygen-starved reaction.
- B) There were external contaminants and/or age-related degradation products in the fuel itself.

RECOMMENDATION

It is recommended that a sample of unused fuel be analyzed as reference sample for comparison with the collected samples of deposits from the subject fuel tank and scavenge pump inlet tube pieces.



Figure 1 Photographs of the tank section CW236 in the as received condition. Figure A shows the inside surface and figures B - D are views of the outside surface. Note a general deformation (curling) of the section.

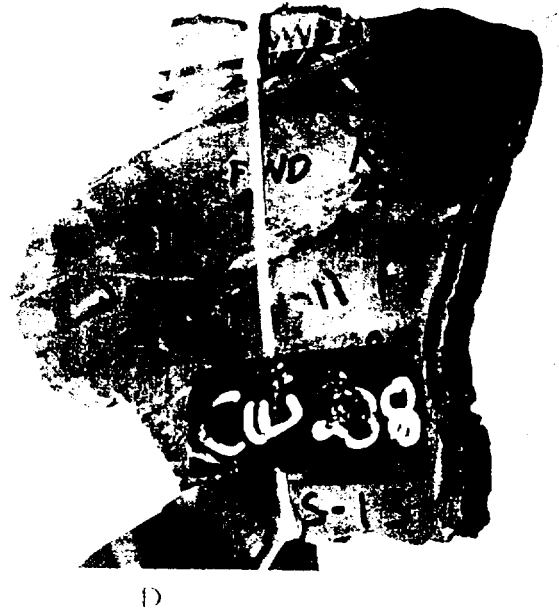
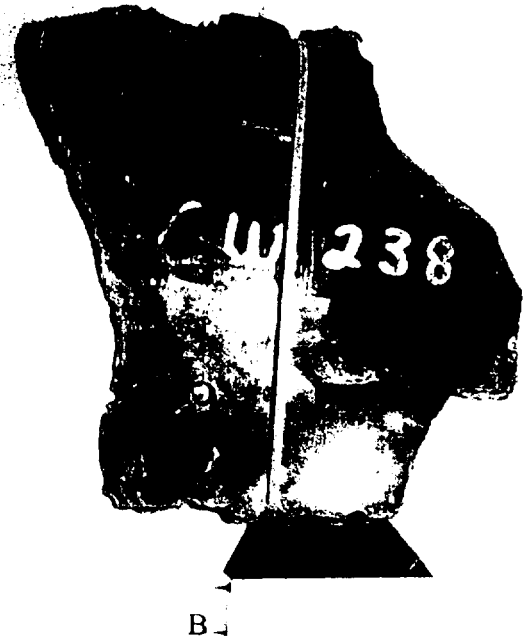


Figure 2 Photographs of the rank section CW 238 in the as-received condition. Figures A & B show the outside surface and figures C & D are views of the inside surface. Note a general deformation of the section. Location of a deep gouge mark is indicated by an arrow in figure A (see figure 1B for details).



A

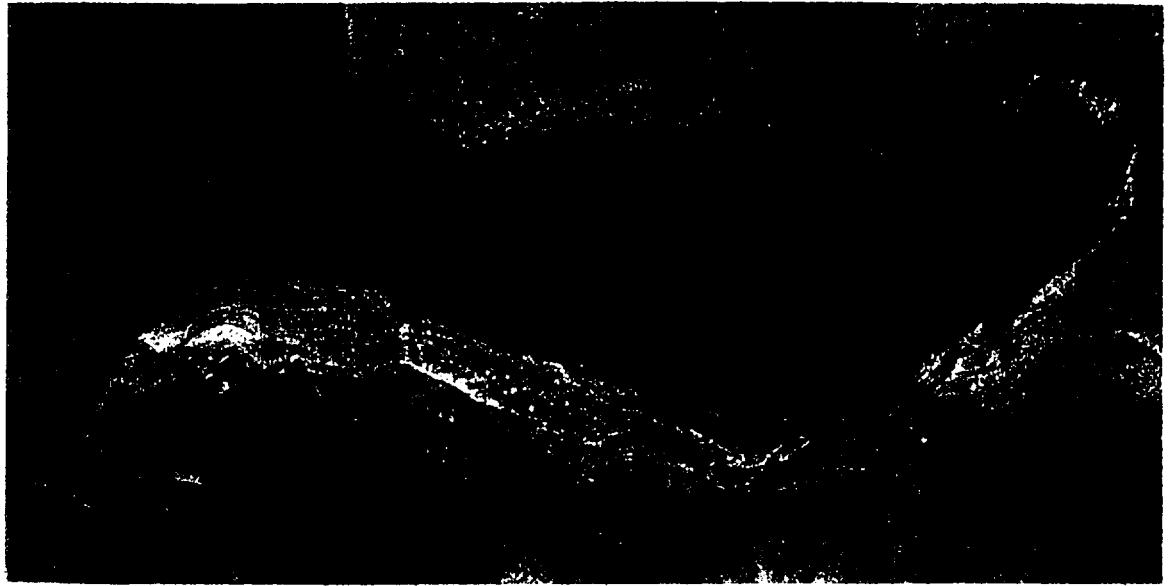


B



C

Figure 3. Photographs of the tank sections show the plane along which the tank had fractured. Figure C exhibits an enlarged view of the fracture in the tank.



A



B

Figure 1 Enlarged photographs of the part of the hole in Section CW236, A - inside surface, B - outside surface

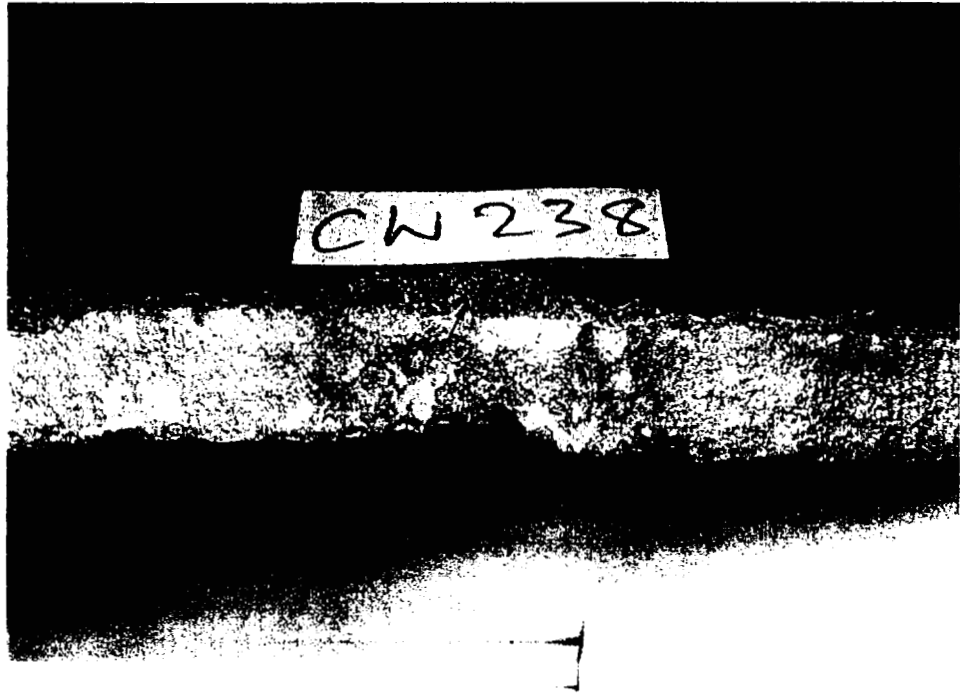


Figure 6A: Photograph of the part of the fracture surface (adjacent to the hole in Section CW236) on Section CW238 shows light brown staining in that area. Note the flattening at the lip of the fracture surface (arrow).

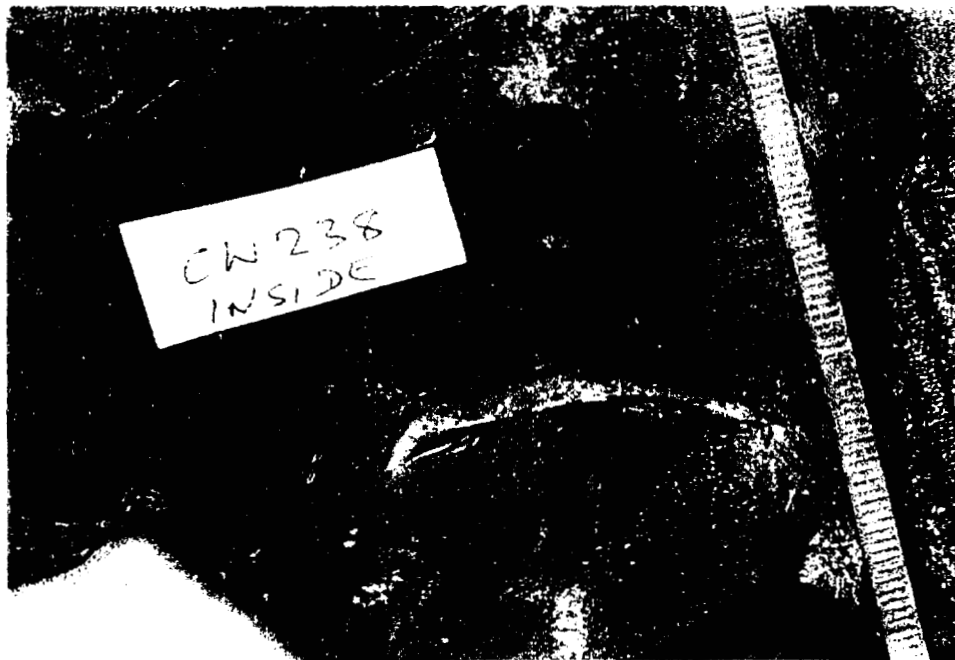


Figure 6B: Photograph of the inside surface of Section CW238 shows a deep gouge mark, about 1.5 inches long.

CW-236
INSIDE

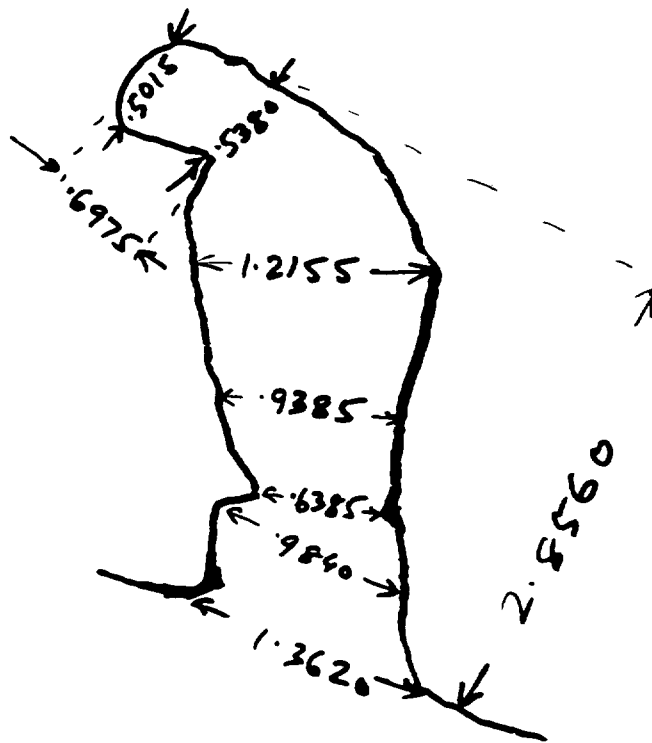


Figure 7A: Profile of the hole in the plane of the inside surface.

CW-236
OUTSIDE

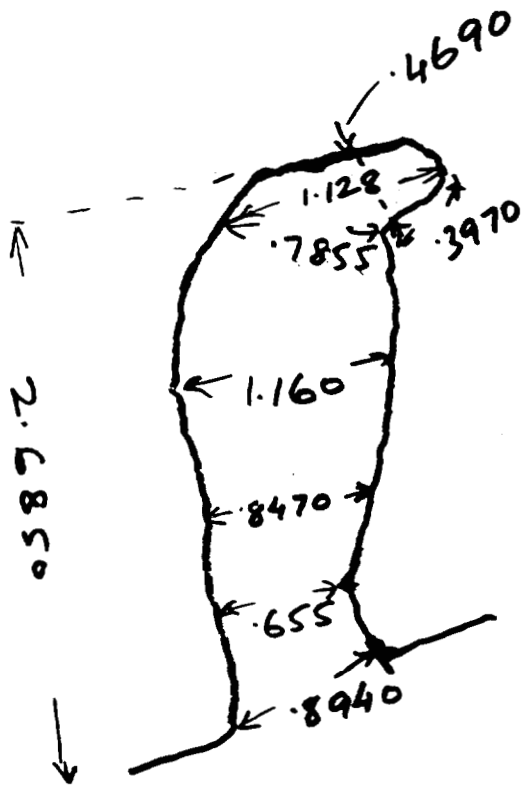


Figure 7B: Profile of the hole in the plane of the outside surface.



Figure 8: Photograph of Section CW236 shows locations of the small sections of the fracture surfaces cut out for analysis.



Figure 9: Photograph of the small sections of Section CW236.



Figure 10: Photograph of the fracture section I cut from Section CW236 shows a two-step failure starting on the inside surface (top). A higher magnification photograph is shown on the right side.

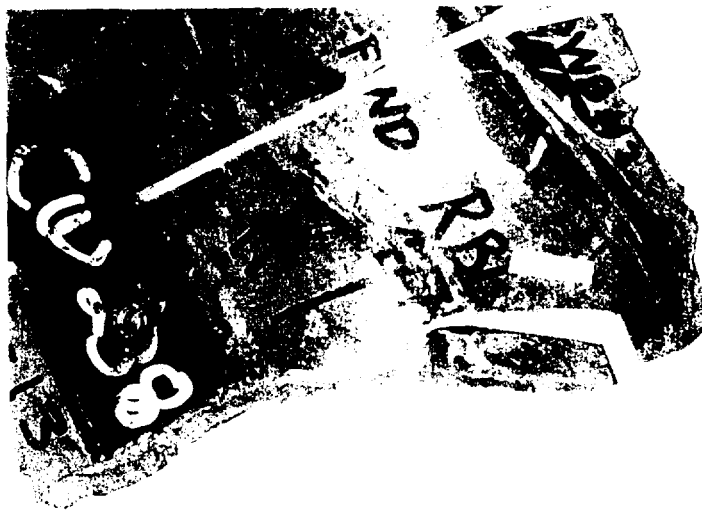


Figure 11: Photograph shows location of the multi-step fracture in Section CW238 for analysis.

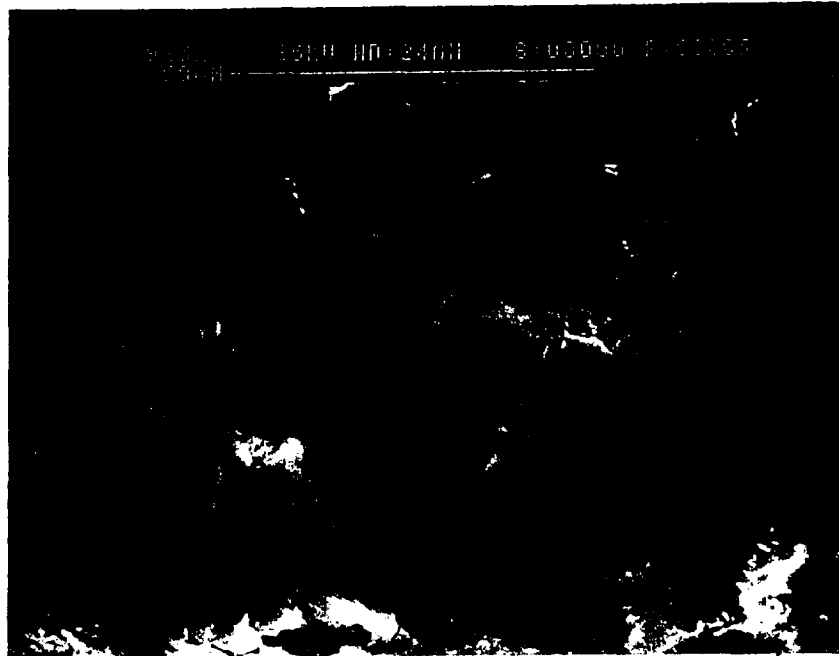


Figure 12: SEM fractograph shows the presence of extensive amounts of corrosion products on the fracture surface. Bottom of the fractograph is toward the inside surface of the tank, X925.

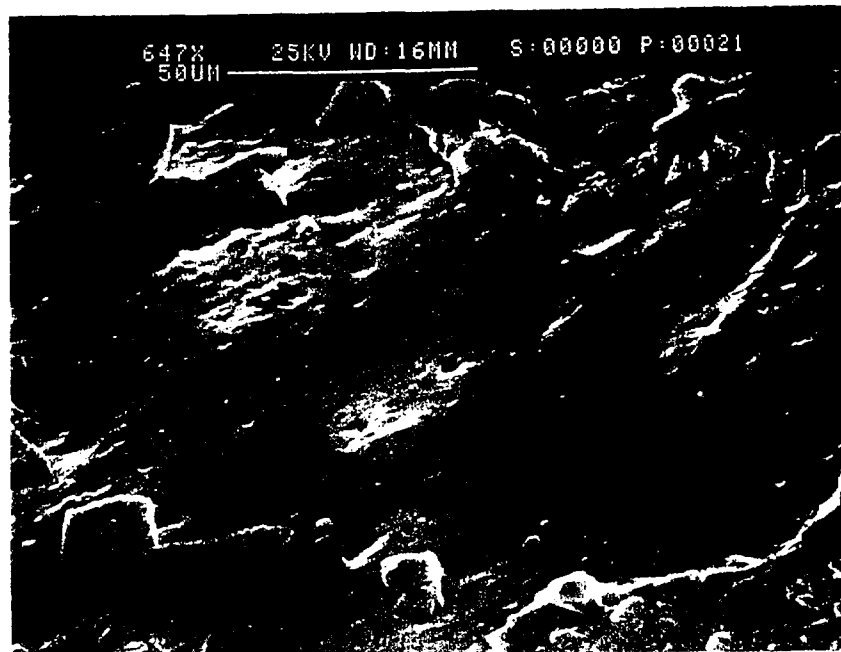


Figure 13: SEM fractograph shows featureless characteristics of the partially cleaned fracture surface. Bottom of the fractograph is toward the inside surface of the tank, X925.

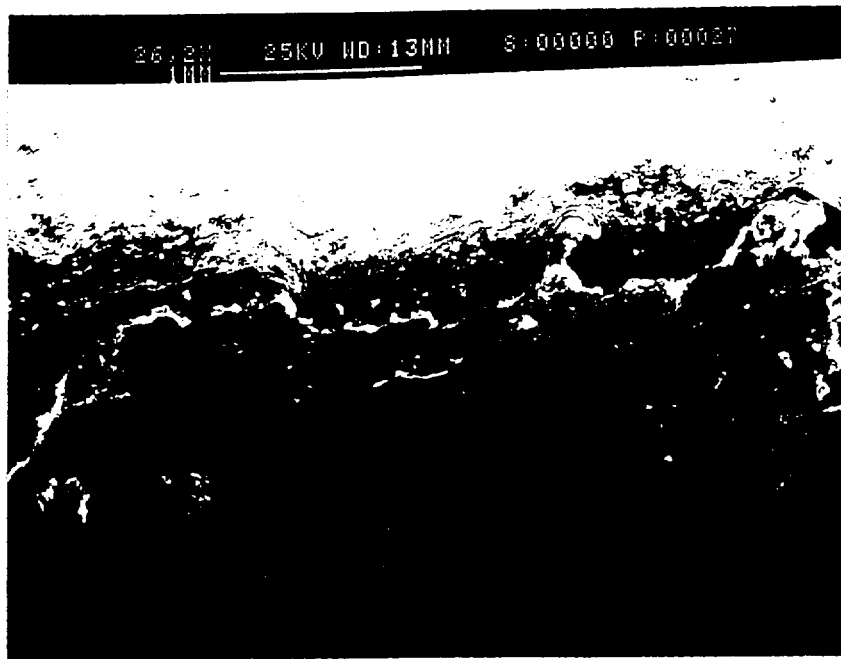


Figure 14: SEM micrograph shows cracking of the paint layer under a tensile load. Top of the fractograph is toward the outside surface of the tank, X26.

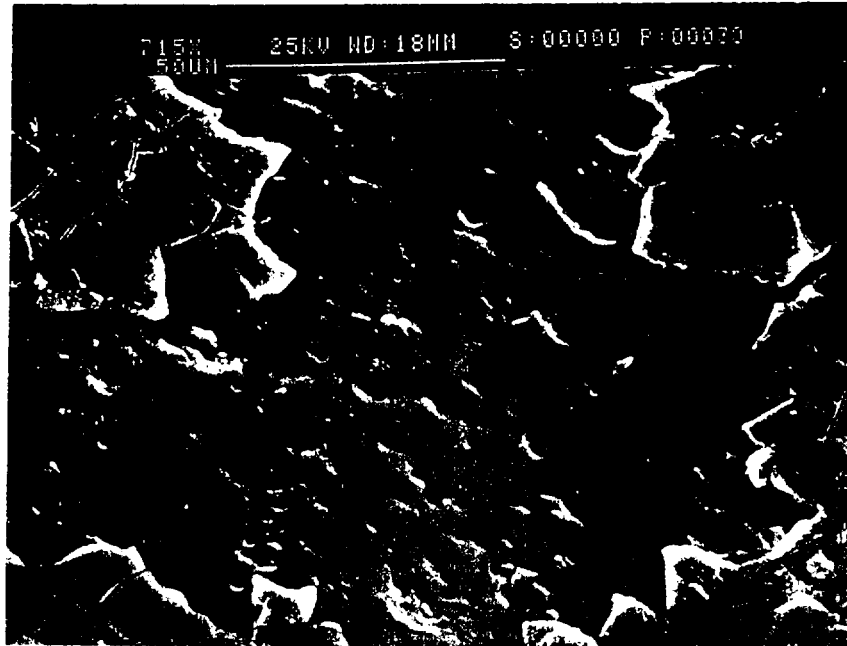


Figure 15: SEM fractograph shows similar features as in figure 14. Bottom of the fractograph is toward the inside surface of the tank, X715.



Figure 16: SEM fractograph shows similar features as in figure 13. Right side of the fractograph is toward the inside surface of the tank, X764.

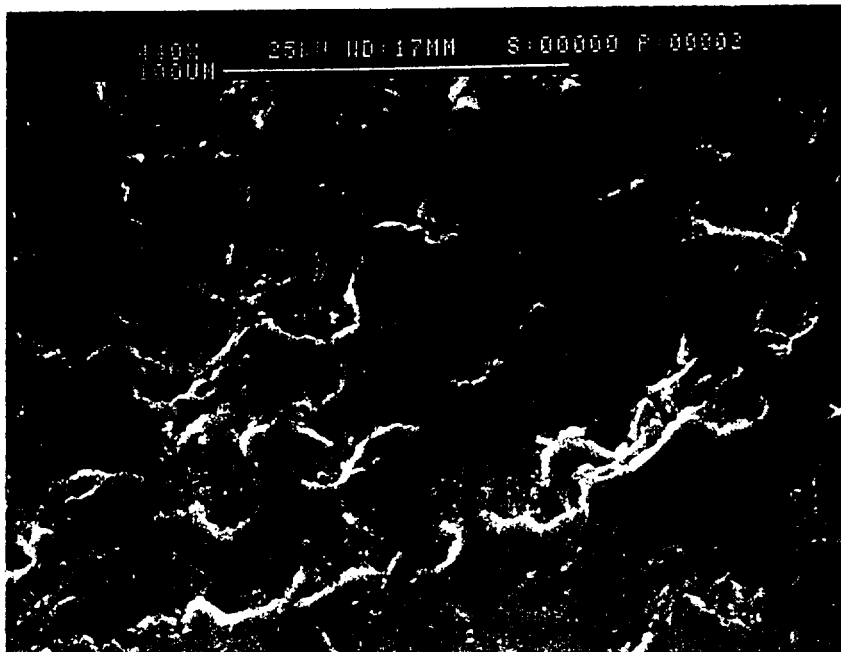


Figure 17: SEM fractograph shows similar features as in figure 12. Bottom of the fractograph is toward the inside surface of the tank, X447.

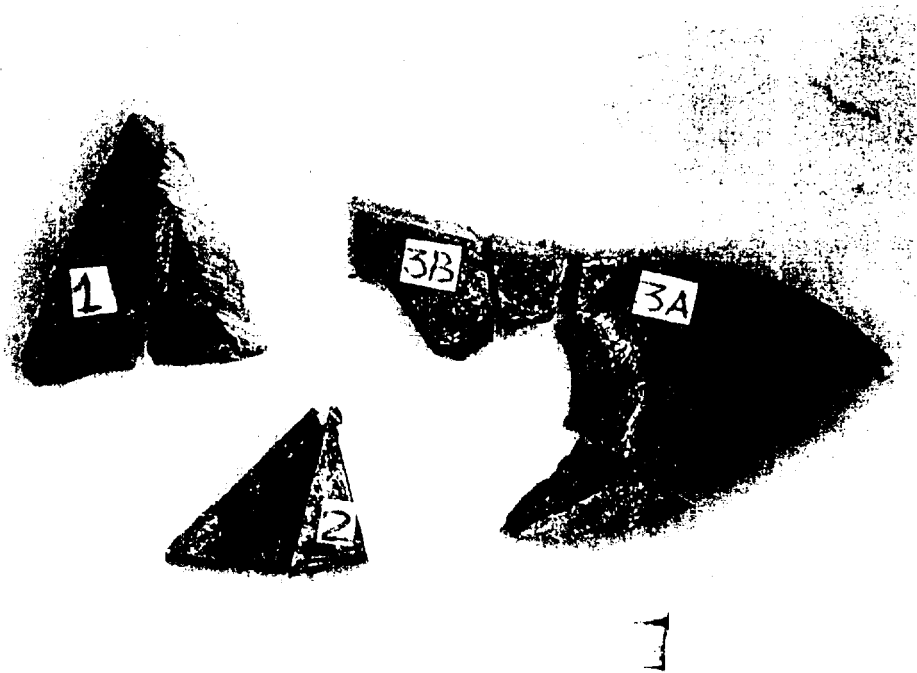
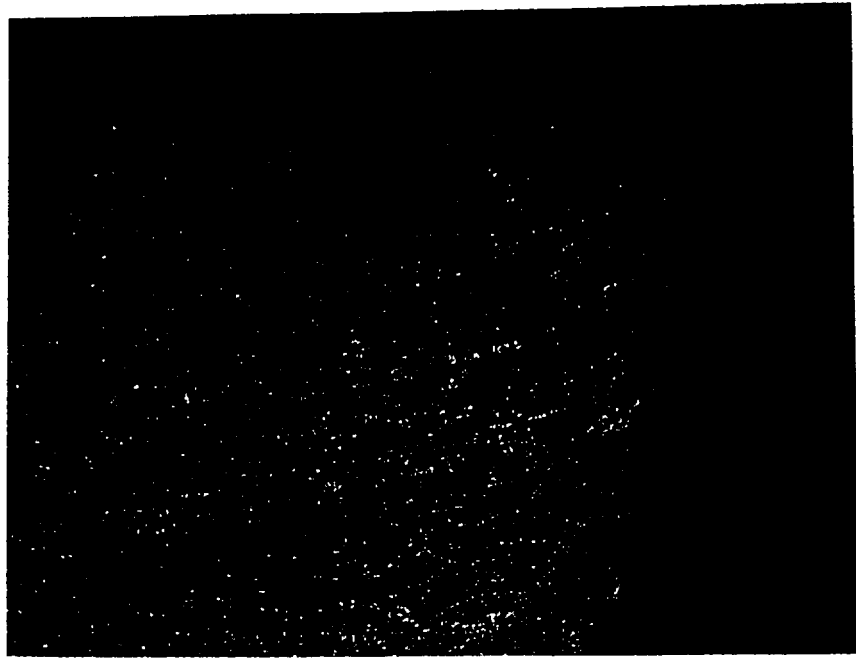


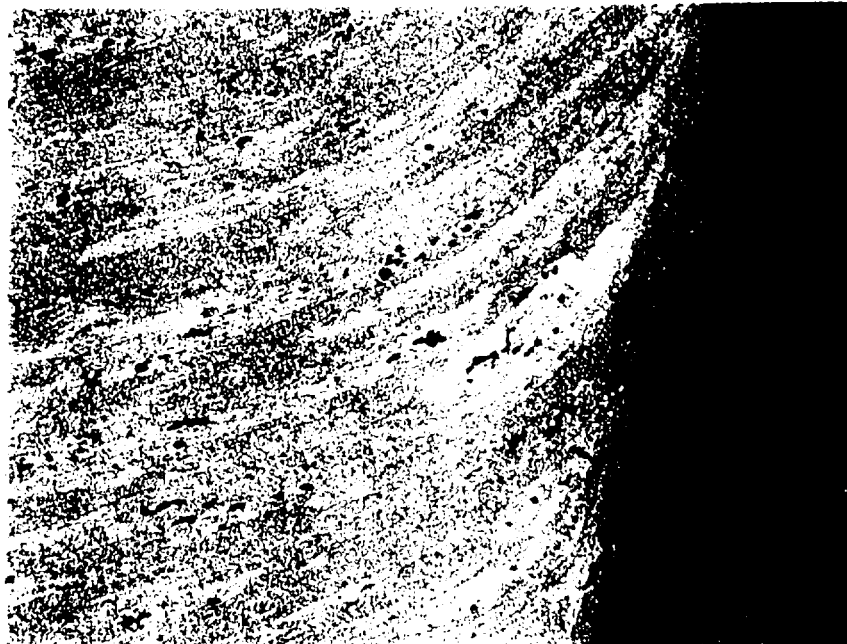
Figure 18: Photograph of the transverse section cut for metallographic analysis of Section CW236



Figure 19: Photograph of the transverse section cut for metallographic analysis of Section CW238

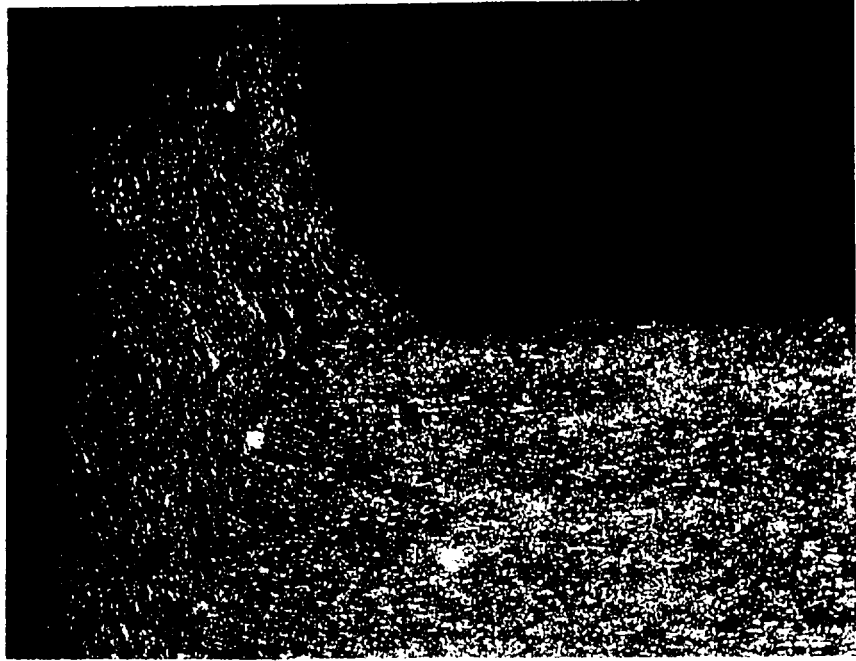


A, X50

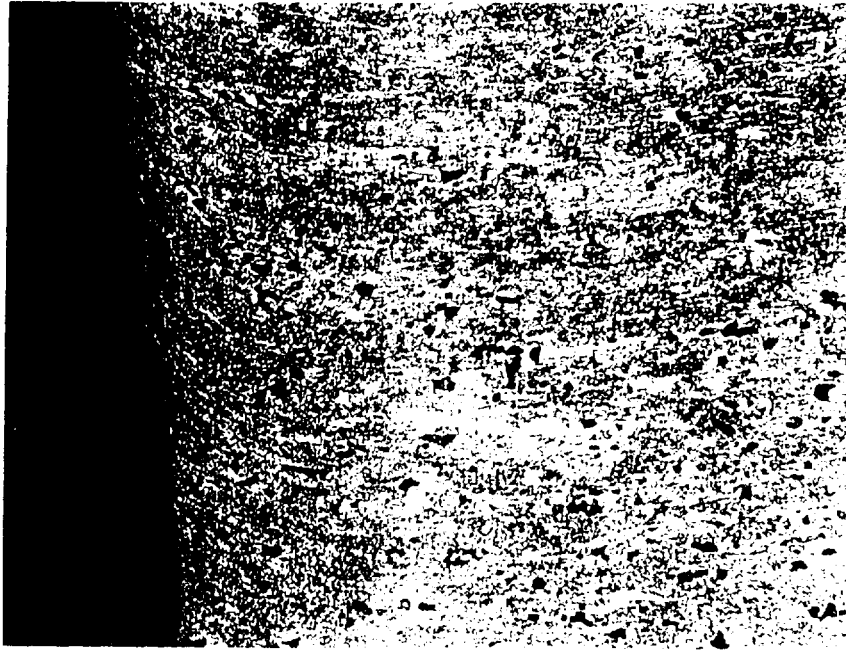


B, X200

Figure 20. Photomicrographs of the polished and etched section CW236-1 show grain flow from the inside surface (bottom of the micrographs) to the outside surface (top of the micrographs). The outside surface in Figure A exhibits evidence of intergranular corrosion, Kojima's etch.

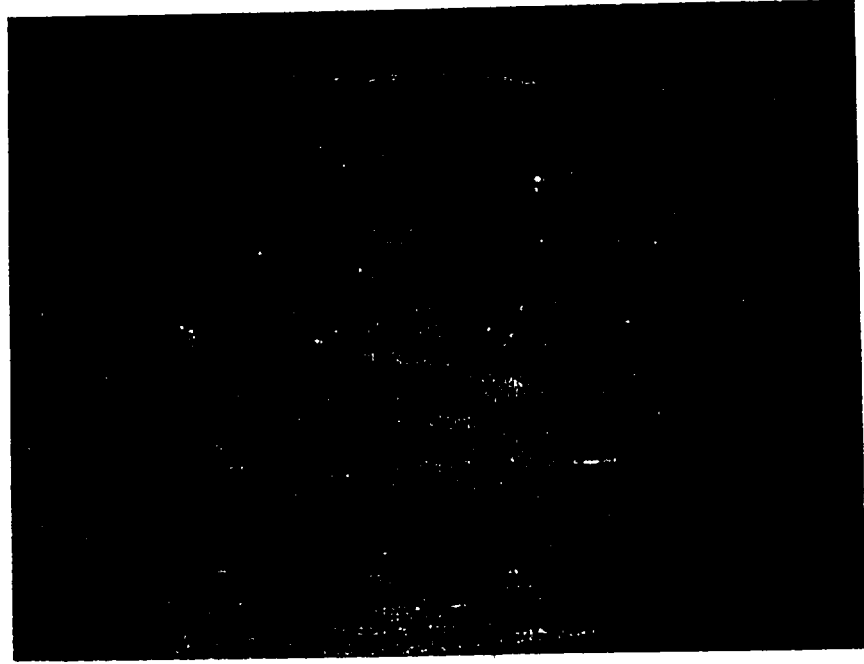


A, X50

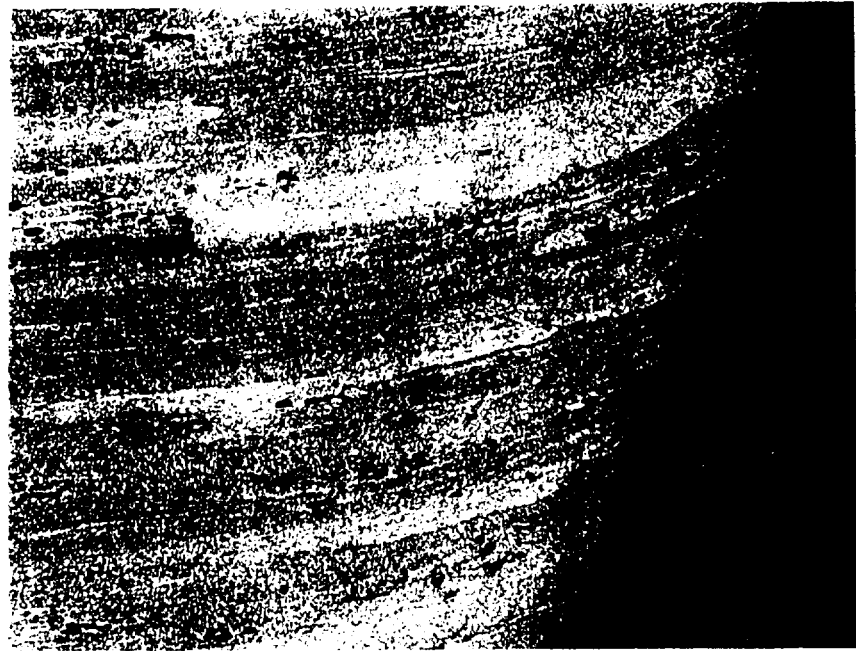


B, X200

Figure 21: Photomicrographs of the polished (not etched) section CW23b - 2 show similar features as in figure 20, Keller's etch.



A, X50

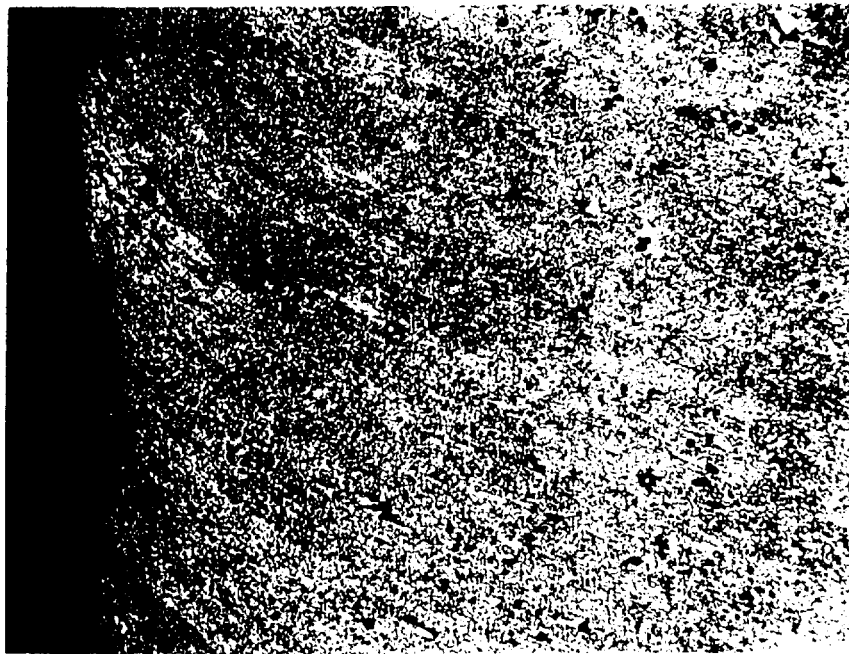


B, X200

Figure 22 Photomicrographs of the polished and etched section CW236. 3A shows similar features as in figure 20. The outside surface in figure A exhibits evidence of intergranular corrosion. Keller's etch.



A, X50

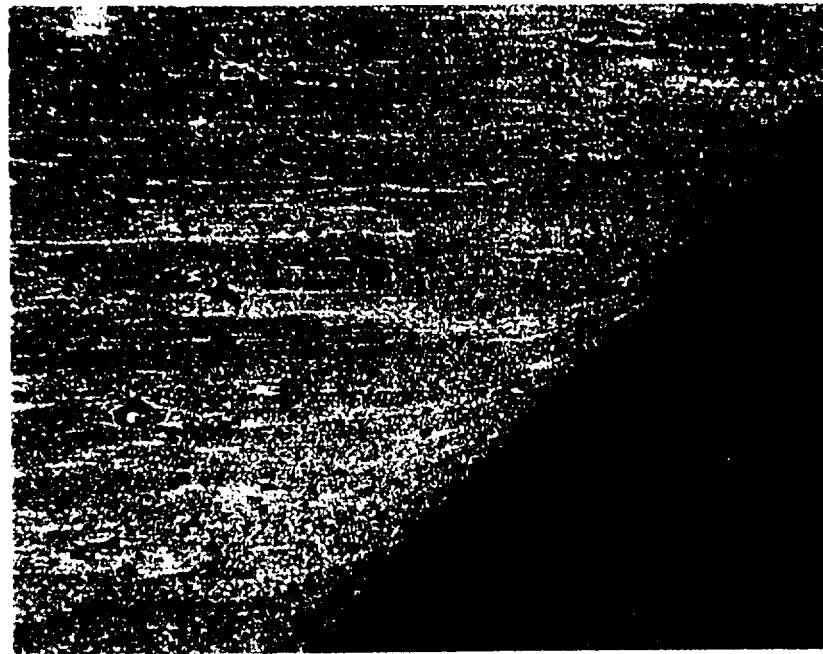


B, X200

Figure 23 Photomicrographs of the polished and etched section CW236. (A) shows similar features as in figure 20. The inside surface in figure A exhibits evidence of intergranular corrosion, Keller's etch.



A, X50

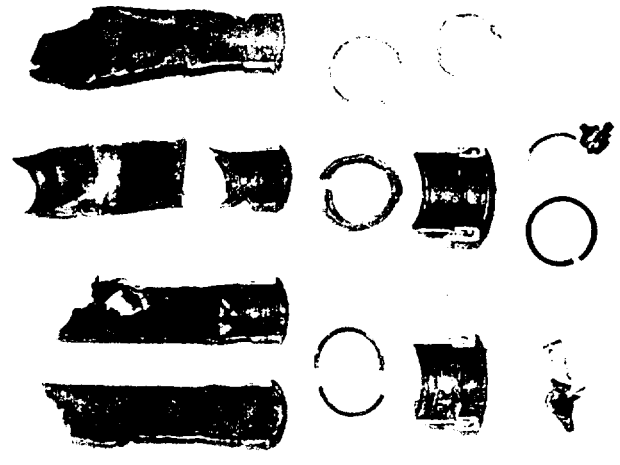


B, X200

Figure 24. Photomicrographs of the polished and etched section CW238 show similar features as in figure 20. The inside surface in figure A exhibits evidence of intergranular corrosion. Keller's etch



A



B

Figure 25. Photographs show the outside and inside surfaces of the pieces of the scavenge pump in the tube. The top two valves and the plunger valve are identical as 85B and the bottom two valves are 85A.

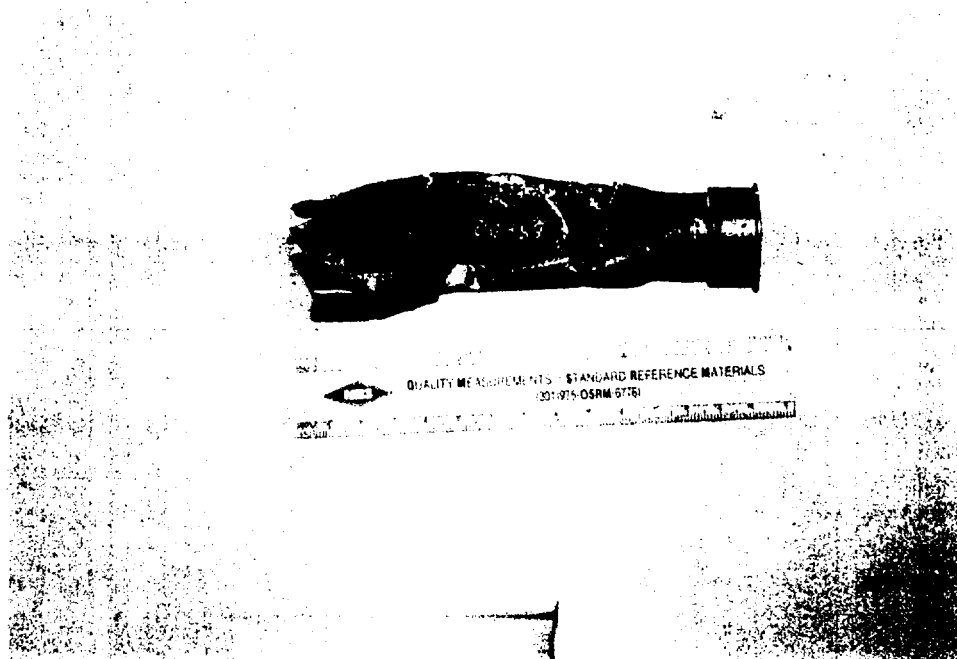


A



B

Figure 5. Photographs of the side view on the side surface of the specimen (Section CW23b) show out void deformation of the surface of (rows).

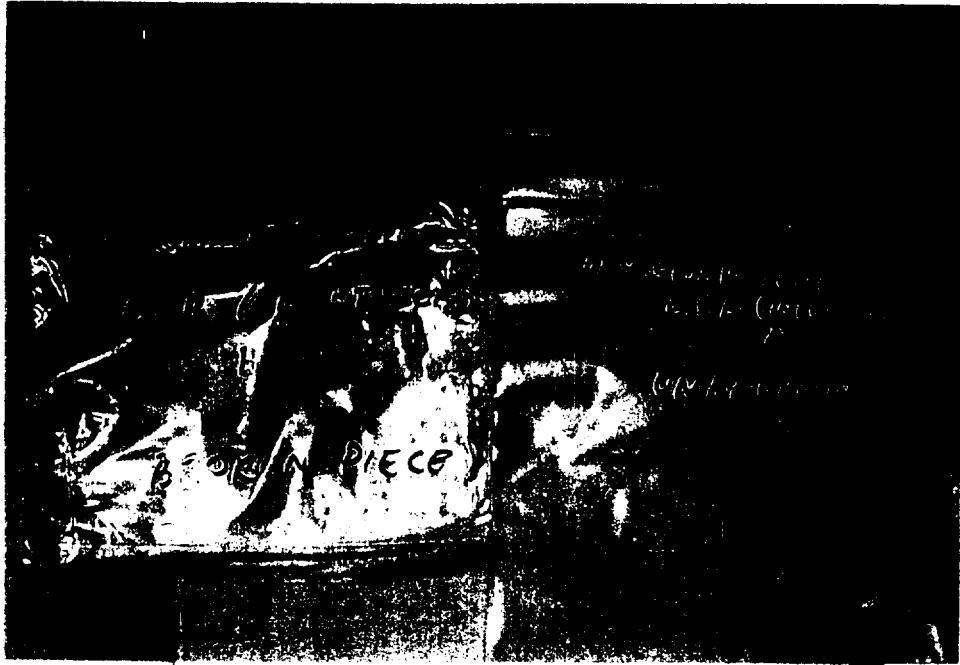


A

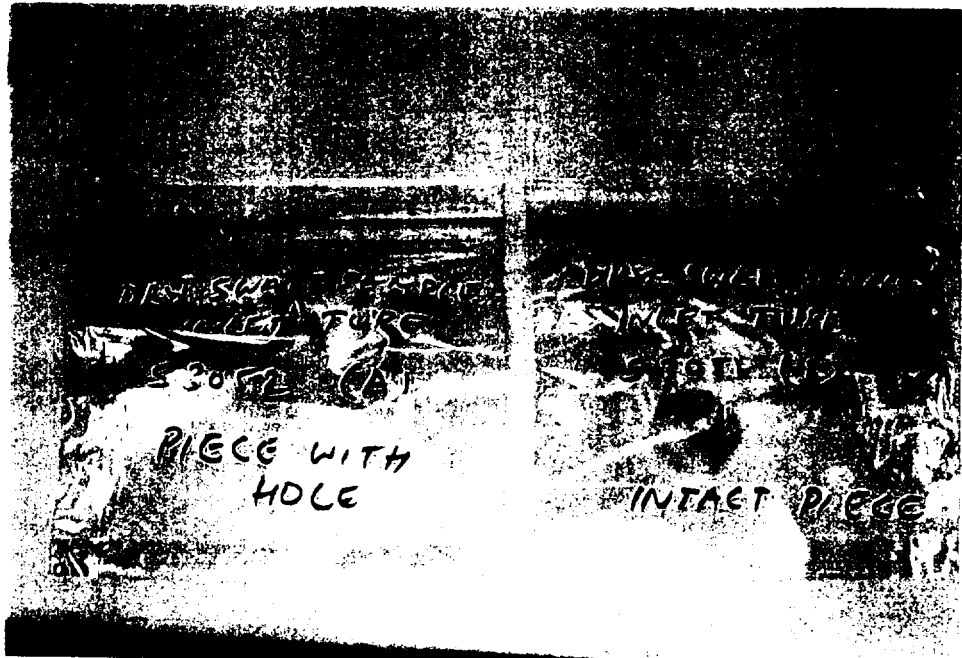


B

Figure 26. Identifications of the tube pieces shown in figure 25 are exhibited clearly in these photographs.



A



B

Figure 27. Dry swab samples are shown in these photographs.

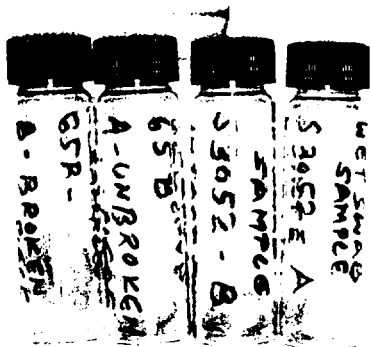


Figure 28. Wet swab samples are shown in this photograph